Available online at www.sciencedirect.com
ScienceDirect
Neuropharmacology 53 (2007) 524–533
NEURO PHARMACOLOGY
www.elsevier.com/locate/neuropharm

Model-specific effects of bumetanide on epileptiform activity in the in-vitro intact hippocampus of the newborn mouse

W. Kilb*, A. Sinning, H.J. Luhmann

Institute of Physiology and Pathophysiology, Johannes Gutenberg University, Duesbergweg 6, D-55128 Mainz, Germany

Received 3 January 2007; received in revised form 21 May 2007; accepted 19 June 2007

Abstract

The immature brain has a higher susceptibility to develop seizures, which often respond poorly to classical pharmacological treatment. It has been recently suggested that bumetanide, which blocks Na^+-dependent K^+-Cl^--cotransporter isoform 1 (NKCC1) and thus attenuates depolarizing GABAergic responses, could soothe epileptiform activity in immature nervous systems. To evaluate whether bumetanide consistently attenuates epileptiform activity, we investigated the effect of 10 μM bumetanide in five different in-vitro epilepsy models using field potential recordings in the CA3 region of intact mouse hippocampal preparations at postnatal day 4–7. Bumetanide reduced amplitude and frequency of ictal-like events (ILE) induced by 8.5 mM K^+, but it increased the frequency of ILE induced by 1 μM kainate. Inhibition of ligand-gated Cl^- channels by 10 μM gabazine and 30 μM strychnine induced interictal activity (IA) that was only marginally affected by bumetanide. Removal of extracellular Mg^{2+} induced both ILE and IA. Bumetanide had no effect on these ILE but enhanced the IA. Low-Mg^{2+} solution containing 20 μM 4-AP induced late-recurrent discharges, which were slightly attenuated by bumetanide. In summary, our results demonstrate that bumetanide exerts diverse effects in different in-vitro epilepsy models.

Keywords: Seizure; Perinatal epilepsy; In-toto preparation; NKCC1; Chloride homeostasis; Immature brain

1. Introduction

Epileptic seizures are one of the most common neurological disorder, with a higher incidence in children compared to adults (Sanchez and Jensen, 2001). Seizures during early childhood can affect mental capabilities and had been attributed as one major risk factor for the development of epilepsy (Holmes, 1997). The higher seizure susceptibility of the immature nervous system (Sanchez and Jensen, 2001) has been attributed to the depolarizing $GABA_A$ receptor mediated responses in immature neurons (Luhmann and Prince, 1991; Holmes et al., 2002). These depolarizing GABAergic responses are probably caused by an elevated intracellular Cl^- concentration ($[Cl^-]_i$) in immature neurons maintained by the activity of the Na^+-dependent K^+-Cl^--cotransporter isoform 1 (NKCC1) (Rohrbough and Spitzer, 1996; Yamada et al., 2004).

It has been recently demonstrated that bumetanide, a blocker of NKCC1, attenuates epileptiform activity induced by elevated extracellular K^+ concentration ($[K^+]_e$) in the immature rodent hippocampus in-vitro and in-vivo (Dzhala et al., 2005). Thus bumetanide would be a candidate for therapeutical interference with childhood epilepsies, where classical pharmacological treatment often fails (Dulac et al., 1995). The antiepileptic effect of bumetanide could not be observed in mice lacking a functional NKCC1 or in the presence of the $GABA_A$ antagonist bicuculline, suggesting that it was caused by reduced Cl^--accumulation and a subsequent shift in $GABA_A$ receptor mediated membrane responses towards inhibition (Dzhala et al., 2005).

* Corresponding author. Tel.: +49 211 392 6101; fax: +49 211 392 6071.
E-mail address: wkilb@uni-mainz.de (W. Kilb).

0028-3908/$ - see front matter © 2007 Elsevier Ltd. All rights reserved.
doi:10.1016/j.neuropharm.2007.06.015

However, Cl^- accumulation mediated by NKCC1 is K^+ dependent and elevated $[K^+]_e$ will therefore artificially raise $[Cl^-]_i$ and may lead to enhanced $GABA_A$-receptor mediated membrane depolarization (Russell, 2000). In addition, bumetanide-mediated attenuation of GABAergic depolarizations diminishes epileptiform activity only under the assumption that GABAergic membrane responses contribute to excitation. But a variety of studies demonstrate that blockade of $GABA_A$ receptors induces epileptiform activity in immature brains under in-vitro and in-vivo conditions (Baram and Snead, 1990; Khalilov et al., 1997b; Wells et al., 2000), suggesting that activation of $GABA_A$ receptors may have inhibitory actions already in the immature brain (Khalilov et al., 1999).

To readress the question whether bumetanide consistently attenuates epileptiform activity, we investigated the effect of bumetanide on various in-vitro epilepsy models. We performed field-potential recordings in intact in-vitro hippocampal preparations of immature C57Bl/6 mice and induced epileptiform activity by elevating $[K^+]_e$, by bath-application of 1 μM kainate, by blockade of $GABA_A$ and glycine receptors, by lowering the extracellular Mg^{2+} concentration and by adding 4-AP to low-Mg^{2+} containing solution. We observed that bumetanide attenuated epileptiform activity in the high $[K^+]_e$ model and in the combined 4-AP/low-Mg^{2+} model, whereas an increased epileptiform activity was observed in the kainate and low-Mg^{2+} model.

2. Methods

2.1. Preparation

All experiments were conducted in accordance with EU directive 86/609/EEC for the use of animals in research and approved by the local ethical committee. We made all efforts to minimize the numbers of animals and their suffering. Neonatal (postnatal day [P] 4–7; day of birth = P0) C57Bl/6 mice were obtained from the local breeding facility and were deeply anesthetized by hypothermia. The brain was quickly removed and immersed for 2–3 min in ice-cold artificial cerebrospinal fluid (ACSF). Subcortical areas were abscised, the hemispheres divided and the hippocampi of both hemispheres carefully isolated from the cerebral cortex (Khalilov et al., 1997a; Moser et al., 2006). Isolated hippocampi were fixed in a submerged chamber (volume 2.2–2.5 ml) where they were continuously superfused with ACSF at a rate of 4–5 ml/min at 31 ± 1 °C. Experiments started after recovery for at least 1 h.

2.2. Data acquisition and analysis

Extracellular field potentials were recorded in the CA3 region of the hippocampus with tungsten electrodes (impedance 4–5 MΩ, FHC, Bowdoinham, ME). Signals were recorded and amplified in AC mode (DPA-2FX, NPI, Tamm, Germany), low-pass filtered at 3 kHz and stored on a PC using an AD/DA board (ITC-16, HEKA, Lamprecht, Germany) and TIDA 4.11 software (HEKA). Extracellular field potentials recorded from up to 4 separate hippocampi were obtained simultaneously and were analyzed independently. Most recordings were analyzed using the program MiniAnalysis 4.3.3 (Synaptosoft, Leonia, NJ). Field potential discharges were identified according to their amplitude and shape by appropriate settings of the parameters in the MiniAnalysis program. The discharges identified by the program were inspected by eye, unless the number of events was >1000 and the error rate in the first 100 inspected events was less than 3%. For further analysis MiniAnalysis datasets were analyzed in an Excel spreadsheet, where single discharges were grouped to bursts according to their inter-discharge interval. Epileptiform activity was characterized by amplitude of discharges, frequency of discharges within epileptiform bursts (calculated from interspike intervals between a discharge and its predecessor), intervals between epileptiform bursts and number of discharges per epileptiform burst. In addition, power spectrograms of epileptiform activity were calculated using a Hamming function (Clampfit 8.1, Axon Instruments, Foster City, CA). For further analysis the power was averaged in four frequency bands (θ: 3–7.5 Hz, α: 7.5–12.5 Hz, β: 12.5–30 Hz and γ: 30–80 Hz). Values were given as mean ± standard error of the mean (SEM). For statistically analysis paired and unpaired two-tailed t-tests were used. Significance was assigned at a level of <0.05.

2.3. Solutions and drugs

ACSF consisted of (in mM): 126 NaCl, 26 $NaHCO_3$, 1.25 NaH_2PO_5, 1 $MgCl_2$, 2 $CaCl_2$, 2.5 KCl, 10 glucose (pH 7.4, osmolarity 316 mOsm). For low-Mg^{2+} solution $MgCl_2$ was replaced by $CaCl_2$. All solutions were equilibrated with 95% O_2/5% CO_2 at least 1 h before use. Bumetanide, gabazine (SR-95531), strychnine and 4-aminopyridine (4-AP) were dissolved in dimethylsulfoxide (DMSO) and added to the solutions shortly before the experiment. The DMSO concentration of the final solution never exceeds 0.2%. Strychnine, gabazine, kainate, 4-AP, bumetanide and DMSO were obtained from Sigma (Taufkirchen, Germany).

3. Results

3.1. High $[K^+]_e$ model

Increasing $[K^+]_e$ of the bathing solution to 8.5 mM induced epileptiform activity in the CA3 region of intact hippocampal preparations after 15.5 ± 1.6 min ($n = 36$). In all preparations the epileptiform activity consisted of ictal-like events (Fig. 1A) starting with a high frequency burst, followed by single burst discharges during the tonic-clonic and clonic phase (Fig. 1B). Ictal-like events appeared with a frequency of 0.008 ± 0.03 Hz, corresponding to an inter-event interval of 117 s. Each ictal-like event consisted on average of 242 ± 19.4 ($n = 36$) single discharges at a frequency of 12.5 ± 1.2 Hz and with an average amplitude of 114 ± 11.4 μV. Power spectrograms revealed that the power during an ictal-like discharge is clearly above baseline levels (Fig. 1C) and that the power of ictal-like activity is stable during the interval used for the pharmacological experiments ($n = 20$, Fig. 1C).

Application of 10 μM bumetanide to the elevated $[K^+]_e$ bathing solution resulted in a slight but significant ($p = 0.003$) reduction in the average amplitude of discharges by 9.9 ± 1.8% ($n = 24$, Figs. 2A–D). In addition, the frequency of ictal-like events was significantly ($p = 0.002$) reduced by 13.3 ± 4.8% ($n = 24$) and the frequency of spikes within an ictal-like event declined by 10.6 ± 4.7% ($p = 0.034$), while the number of discharges within an ictal-burst was unaffected (Fig. 2D). Bumetanide also reduced the power of ictal-like events (Fig. 2E), which were significantly ($p < 0.05$) lower in the θ-, α- and β-frequency bands (Fig. 2F). In control experiments without bumetanide application ($n = 20$), ictal-like events were not significantly affected during the recording interval of 60 min, except of a significant ($p = 0.02$) decrease in θ-frequency range by 9.9 ± 0.9% (data not shown). In summary, these results demonstrate that bumetanide reduces several parameters of the ictal-like events in the high $[K^+]_e$

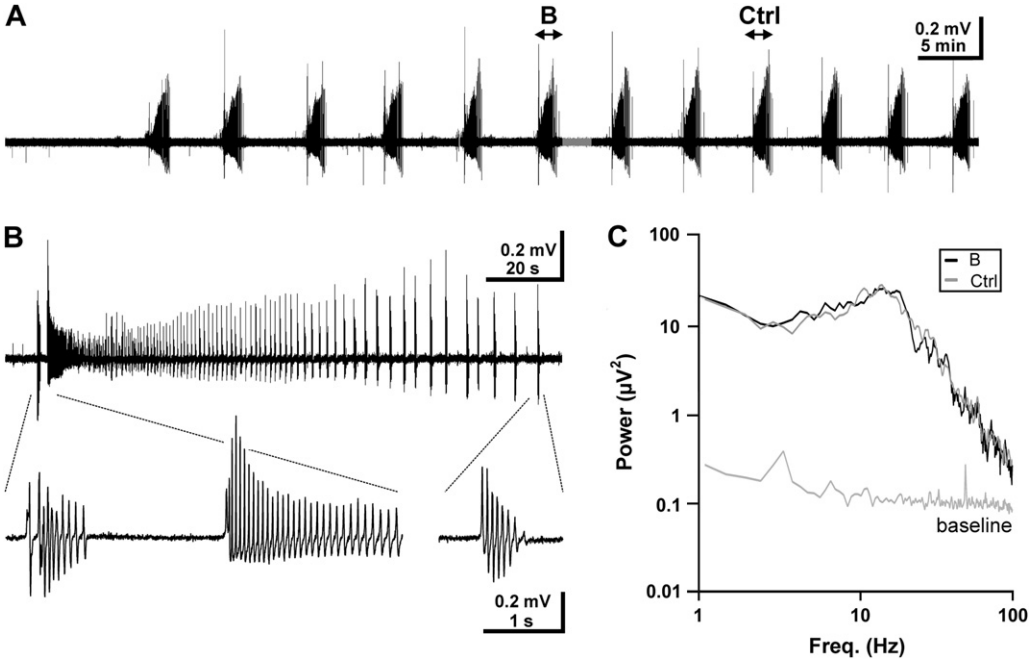

Fig. 1. Epileptiform activity induced by elevated $[K^+]_e$. A: Field-potential recording in the CA3 region of an intact hippocampal preparation from a P6 mouse. Application of 8.5 mM $[K^+]_e$ solution induced repetitive ictal-like events (ILE). B: One ILE, as marked in A, displayed at higher temporal resolution. Initial burst and one of the bursts in the clonic phase are displayed at higher temporal resolution below the trace. C: Power spectrogram of the baseline trace (as calculated from the gray-colored section of the recording shown in A), of the ILE shown in B (black trace) and of one ILE occurring in the interval used for bumetanide application in further experiments (Ctrl, gray trace). Note that the power spectrograms of both ILEs are similar and clearly above baseline levels.

model, suggesting that this substance can attenuate epileptiform activity.

3.2. Disinhibition model

Next we examined the effect of bumetanide after complete blockade of ligand-gated Cl^- channels. Therefore we did not only inhibit $GABA_A$ receptors, but additionally blocked glycine receptors, which contribute to suppression of epileptiform activity in the hippocampus (Kirchner et al., 2003). Simultaneous inhibition of both $GABA_A$ and glycine receptors using 10 μM gabazine and 30 μM strychnine induced epileptiform activity after surprisingly short application time. In the majority of the preparations (27 out of 34) epileptiform activity started after 2.8 ± 0.3 min with one or two ictal-like events and subsequently converted into repetitive interictal activity (Fig. 3A). The initial ictal-like event lasted for 21.4 ± 1.5 s ($n = 27$) and consisted of 99.7 ± 7.5 single discharges occurring at a frequency of 4.4 ± 0.26 Hz (Fig. 3B). In the remaining 7 of the 34 investigated hippocampi epileptiform activity started directly with interictal activity 5.3 ± 0.3 min after application of gabazine/strychnine. Interictal bursts occurred at an average frequency of 0.046 ± 0.003 Hz ($n = 34$), corresponding to an interval of 21.7 s. Each interictal burst consisted of 4.6 ± 0.4 ($n = 34$) single discharges with an average amplitude of 301 ± 35 μV occurring at a frequency of 11.4 ± 0.7 Hz (Fig. 3C).

Application of 10 μM bumetanide to the gabazine/strychnine containing bathing solution slightly reduced the amplitude of epileptiform discharges, while other properties of the interictal activity remained unaltered (Figs. 3D–F). Statistical analysis revealed, that bumetanide application significantly ($p = 0.0009$) reduced the amplitude of epileptiform discharges by $8.3 \pm 1.6\%$ ($n = 22$), but had no significant effect on the number of discharges per interictal burst, the frequencies of interictal bursts and on the frequencies of discharges within an interictal burst (Fig. 3G). In addition, bumetanide had no significant effect on the power of epileptiform activity (Fig. 3H) in θ-, α-, β- and γ-frequency range (Fig. 3I). In control experiments without bumetanide application ($n = 20$), interictal activity was not significantly affected during the recording interval of 60 min (Fig. 3G). In summary, these results demonstrate that bumetanide has only little effect on interictal discharges in the disinhibition epilepsy model of the hippocampus, suggesting that $GABA_A$ and glycine receptors may be necessary to mediate the bumetanide effects.

3.3. Low-Mg^{2+} model

Although the previous sets of experiments demonstrated that bumetanide can attenuate high K^+-induced epileptiform activity and has only a marginal effect in the presence of $GABA_A$ and glycine receptor antagonists, the conclusions from these experiments are somewhat hampered by the fact that elevated $[K^+]_e$ increases the driving force for Cl^- uptake and may thus artificially alter $[Cl^-]_i$ and $GABA_A$ reversal potential (Korn et al., 1987). In addition, the interictal-like epileptiform activity induced by $GABA_A$ and glycine receptor

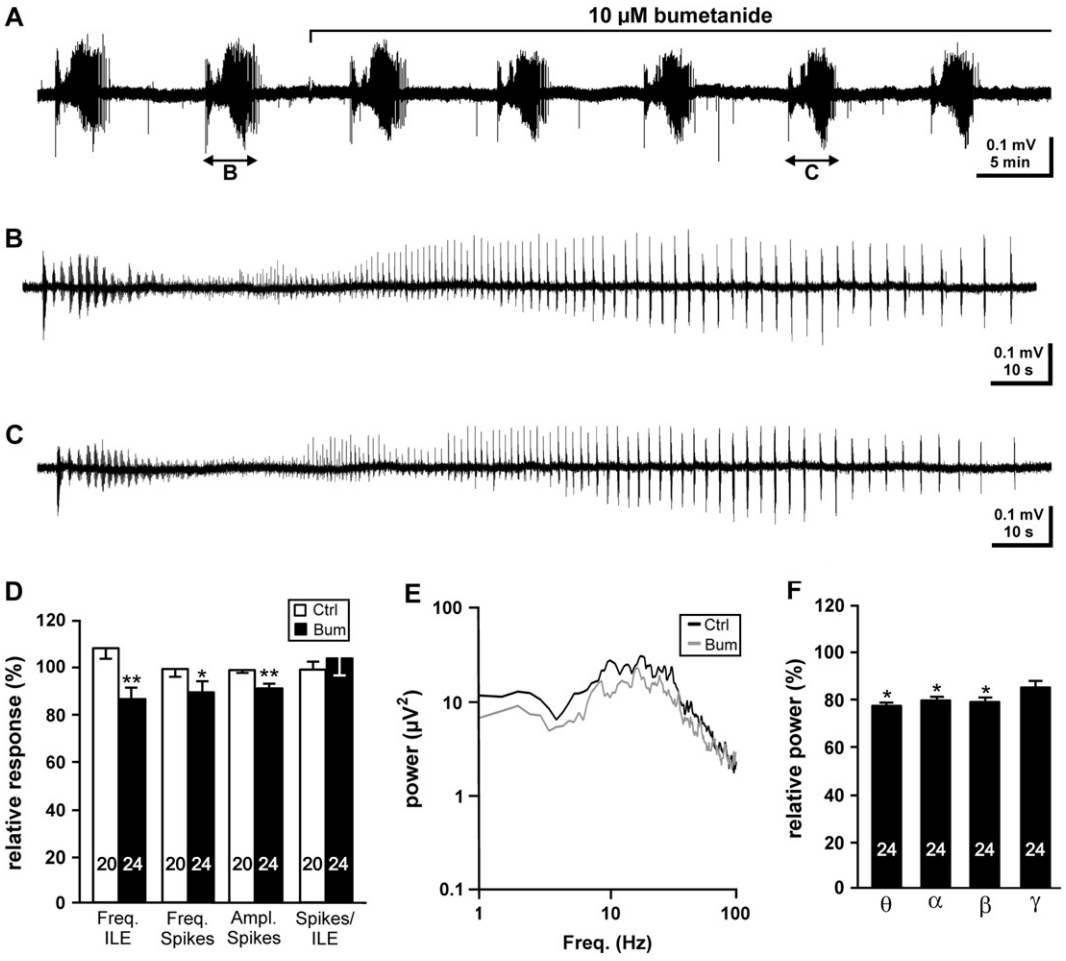

Fig. 2. Effect of bumetanide on epileptiform activity induced by elevated $[K^+]_e$. A: Field potential recording of ictal-like events (ILE) induced by elevated $[K^+]_e$ in the CA3 region of an intact hippocampal preparation from a P6 mouse. Application of 10 µM bumetanide slightly reduced the amplitude of ILE. The ILEs marked with B and C are displayed in higher temporal resolution in panel B and C. D: Statistical analysis of the bumetanide effects on different parameters of epileptiform activity. Control experiments (open bars) revealed that the properties of ILE were unaltered in the interval used for bumetanide application. Bumetanide (filled bars) significantly reduced the frequency of ILE, the frequency of discharges within an ILE and the amplitude of discharges. E: Power spectrogram of the control ILE shown in B (black line) and the ILE shown in C after bumetanide application (gray line). Note that bumetanide attenuated the power. F: Statistical analysis of the relative power, as compared to control ILEs, in various frequency ranges. Bumetanide significantly reduced the power in the θ-, α-, and β-frequency range. Bars represent mean ± SEM. Numbers of experiments are indicated in the bars.

antagonists has completely different properties than the ictal-like events induced by elevated $[K^+]_e$ and it is not clear whether bumetanide will effect interictal-like activity already in the presence of $GABA_A$- and glycine-mediated synaptic currents. To address these questions we analyzed the effect of bumetanide on epileptiform activity induced by low-Mg^{2+} solution, since it has been demonstrated that under these conditions both ictal-like and interictal-like activity were elicited in the intact hippocampal preparation of immature mice (Moser et al., 2006).

In 35 of the 47 investigated hippocampi epileptiform activity started 10 ± 1.0 min after the switch to low-Mg^{2+} solution with interictal activity, while in the remaining preparations epileptiform activity started with ictal-like events after 16.8 ± 1.5 min ($n = 13$). Most of the hippocampi (32 out of 47) showed both interictal- and ictal-like activity (Fig. 4A), while 12 hippocampi showed only interictal activity and 3 only ictal-like events. Interictal activity had an average frequency of 0.074 ± 0.009 Hz ($n = 44$), corresponding to an interval of 13.5 s. Each interictal burst consisted of 2.2 ± 0.2 ($n = 44$) single discharges with average amplitude of 119.4 ± 8.6 µV, occurring at a frequency of 18.6 ± 2.2 Hz (Fig. 4B). Ictal-like event lasted for 78.5 ± 10.6 s ($n = 35$) and consisted of 139 ± 12.7 discharges at a frequency of 10.3 ± 0.72 Hz and with average amplitude of 86.7 ± 7.8 µV (Fig. 4C). Repetitive ictal-like events were observed in 23 hippocampi at an average frequency of 0.008 ± 0.0049 Hz.

Application of bumetanide had no obvious effect on low-Mg^{2+} induced ictal-like activity (Fig. 4D). The amplitude, the number of discharges per ictal-like event, the frequency of discharges within an ictal-like event and the frequency of ictal-like events were not significantly affected ($n = 12$, Fig. 4E). In addition, the power of ictal-like events in the θ-, α- and β-frequency range was not significantly altered by bumetanide, while the power in the γ-frequency range was significantly increased by 30 ± 3.4% ($n = 12$) (Fig. 4F).

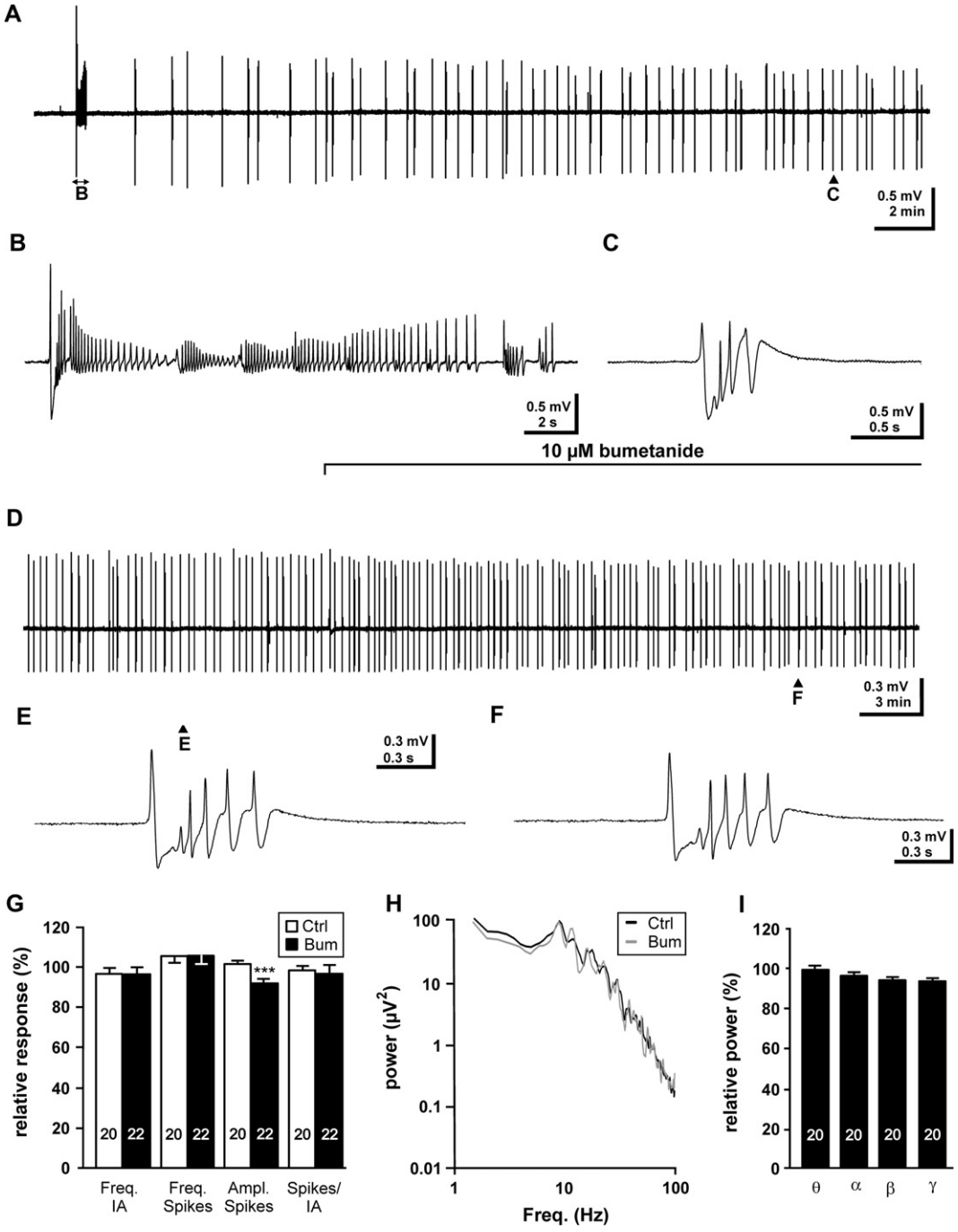

Fig. 3. Effect of bumetanide on epileptiform activity induced by inhibition of $GABA_A$ and glycine receptors. A: Field-potential recording in the CA3 region of an intact hippocampal preparation from a P4 mouse. Combined application of 10 µM gabazine and 30 µM strychnine induced one initial ictal-like event (ILE) and subsequent repetitive interictal activity (IA). B: The initial ILE shown in higher temporal resolution. C: One interictal burst, as marked in A, displayed in higher temporal resolution. D: Field potential recording in the CA3 region of an intact hippocampal preparation from a P5 mouse demonstrating the effect of 10 µM bumetanide on IA. Note the slight amplitude reduction in the presence of bumetanide. The interictal bursts marked by arrowheads are displayed in higher temporal resolution in E and F. G: Statistical analysis of bumetanide effects on different parameters of IA. Control experiments (open bars) revealed that the properties of ILE were unaltered in the interval used for bumetanide application. Bumetanide (filled bars) significantly reduced the amplitude of IA while the other parameters were not affected. H: Power spectrogram of IA recorded before (Ctrl, black line) and during the application of 10 µM bumetanide (Bum, gray line). F: Statistical analysis of the relative power, as compared to the control interval before bumetanide application. Bumetanide had no significant effect on the power in the analyzed frequency range. Bars represent mean ± SEM. Numbers of experiments are indicated in the bars.

In contrast, 10 µM bumetanide had a clear effect on the interictal activity (Figs. 4G,H). While the frequency of interictal events, the frequency of discharges within an interictal burst and their amplitude remained unaltered in bumetanide, the number of discharges per events was significantly ($p = 0.018$) increased to 3.4 ± 0.5 ($n = 21$, Fig. 4H), corresponding to $136.4 \pm 11.1\%$ (Fig. 4I). This increased number of spikes leads to an enhanced power of interictal epileptiform activity. In the

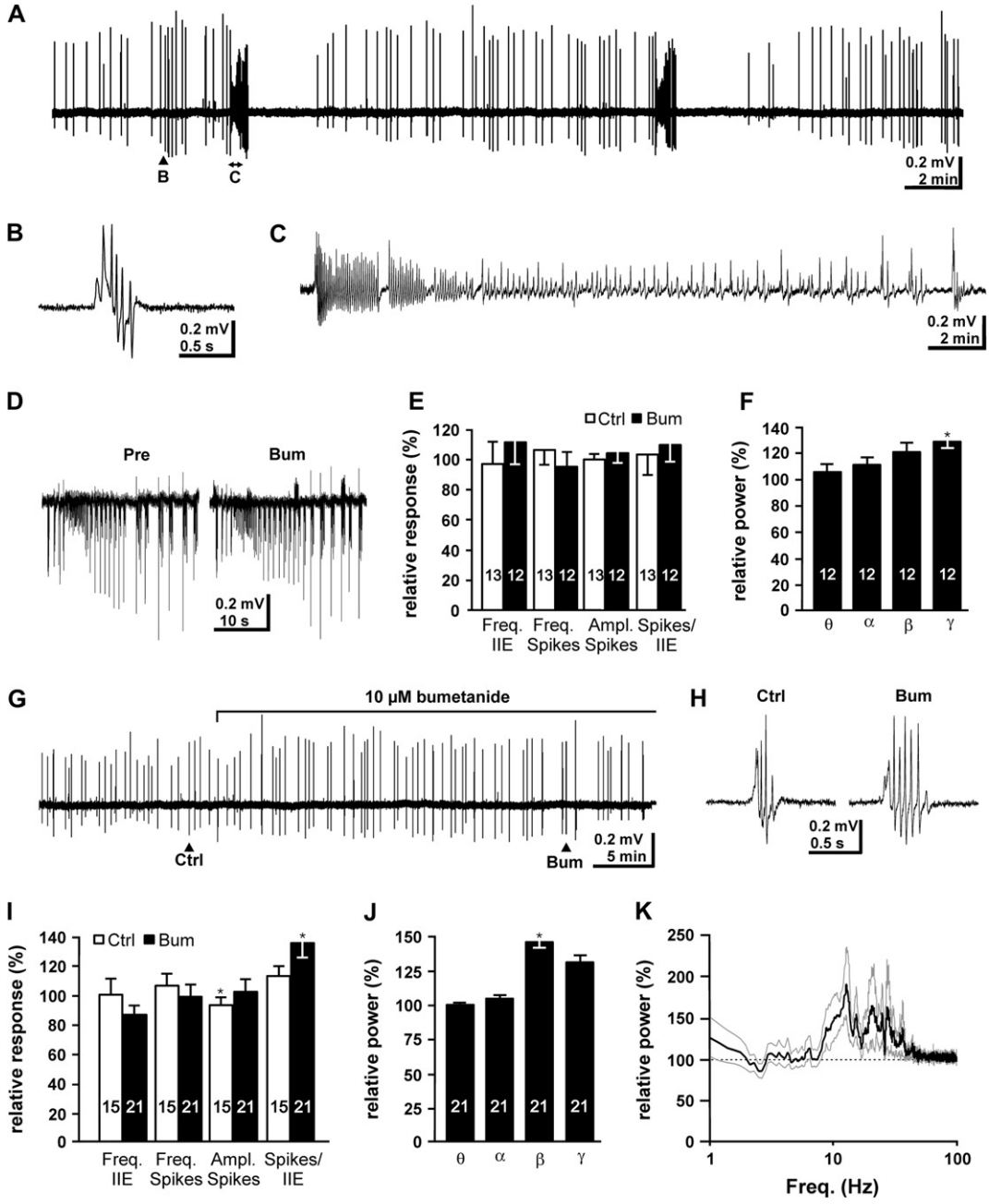

Fig. 4. Effect of bumetanide on low-Mg^{2+} induced epileptiform activity. A: Field-potential recording in the CA3 region of an intact hippocampal preparation from a P5 mouse. In low-Mg^{2+} solution both ictal-like events (ILE) and interictal activity (IA) were observed. B: One interictal burst, as marked in A, shown in higher temporal resolution. C: The initial discharges of an ILE, as marked in A, in higher temporal resolution. D: Subsequent recordings of low-Mg^{2+} induced ILE before and after the application of 10 μM bumetanide. E: Statistical analysis of bumetanide effects on different parameters of ILE. The properties of ILE were not altered in control experiments (open bars) and in the presence of bumetanide (filled bars). F: Statistical analysis of the relative power of ILE, as compared to control ILE before bumetanide application, in various frequency ranges. Bumetanide significantly increased the power in the γ-frequency range. G: Field potential recording displaying the effect of 10 μM bumetanide on low-Mg^{2+} induced IA. H: Interictal bursts, as marked in G, recorded before (Ctrl) and after the application of 10 μM bumetanide (Bum) in higher temporal resolution. Note that the number of discharges within a burst increased in the presence of bumetanide. I: Statistical analysis of bumetanide effects on different parameters of IA. While control experiments (open bars) revealed that the properties of ILE were unaltered in the interval used for bumetanide application, bumetanide (filled bars) significantly increased the number of discharges per interictal burst. J: Statistical analysis of the relative power, as compared to the IA before bumetanide application. Bumetanide significantly increased the power in the β-frequency range. K: Spectrogram displaying the average relative power of IA from 21 experiments (thick line ± SEM indicated by thin, gray lines) after application of 10 μM bumetanide. Note the increase in the relative power above 10 Hz. Bars represent mean ± SEM. Numbers of experiments are indicated in the bars.

presence of bumetanide the power of interictal activity in the β-frequency range was significantly ($p = 0.02$) increased by $46 \pm 4.1\%$ ($n = 21$), while the power in the other frequency ranges was not significantly altered (Figs. 4J,K). In control experiments, without bumetanide application, the properties of ictal-like events ($n = 13$) were not significantly affected during the recording interval of 60 min, while the amplitude of interictal activity slightly ($p = 0.035$) decreased over time

($-6.8 \pm 5.4\%$, $n = 15$, data not shown). In summary, these results demonstrate that bumetanide did not attenuate low-Mg^{2+} induced epileptiform activity but instead enhanced interictal activity.

3.4. Kainate model

To gather more information on the effect of bumetanide on ictal-like epileptiform activity, we also investigated the effect of bumetanide on ictal-like epileptiform activity evoked by the excitotoxin kainate (Khalilov et al., 1999). Bath-application of 1 μM kainate induced ictal-like activity in the CA3 region of intact hippocampal preparations (Fig. 5A) that started 16.7 ± 3.2 min ($n = 32$) after kainate application. Ictal-like events appeared with a frequency of 0.006 ± 0.0008 Hz, corresponding to an average inter-event interval of 164 s. Each ictal-like event consisted on average of 141 ± 15 ($n = 32$) single discharges at a frequency of 11.6 ± 0.9 Hz and with an average amplitude of 99.3 ± 12.1 μV.

Application of 10 μM bumetanide to kainate-containing bathing solution significantly ($p = 0.006$) increased the frequency of ILE to $279.5 \pm 57.3\%$ of the values under control conditions ($n = 17$, Figs. 5B,C). The amplitude, frequency and number of spikes within an ictal-like event remained unaffected. This increased occurrence of ictal-like epileptiform bursts was reflected by an enhanced power (Fig. 5D), which was significantly ($p < 0.05$) higher in θ-, α- and β-frequency bands (Fig. 5E). In control experiments without bumetanide application ($n = 15$), the properties and the power spectrograms of ictal-like events were not significantly affected during the recording interval of 60 min. In summary, these results demonstrate that bumetanide increased the frequency and power of kainate-induced ictal-like events, suggesting that in this model bumetanide enhances epileptiform activity.

3.5. 4-AP/low-Mg^{2+} model

To evaluate the effects of bumetanide on various types of epileptiform activity, we also investigated late recurrent discharge (LRD) activity, which can be induced in the immature hippocampus by the combination of the 4-AP and low-Mg^{2+} model (Kilb et al., 2006). After washing of 20 μM 4-AP containing low-Mg^{2+} solution epileptiform activity started with a long lasting burst of discharges, reminiscent to ictal-like activity, which gradually transformed into repetitive short bursts typical for LRD activity (Fig. 6A). These repetitive bursts occurred at a frequency of 0.32 ± 0.29 Hz ($n = 38$)

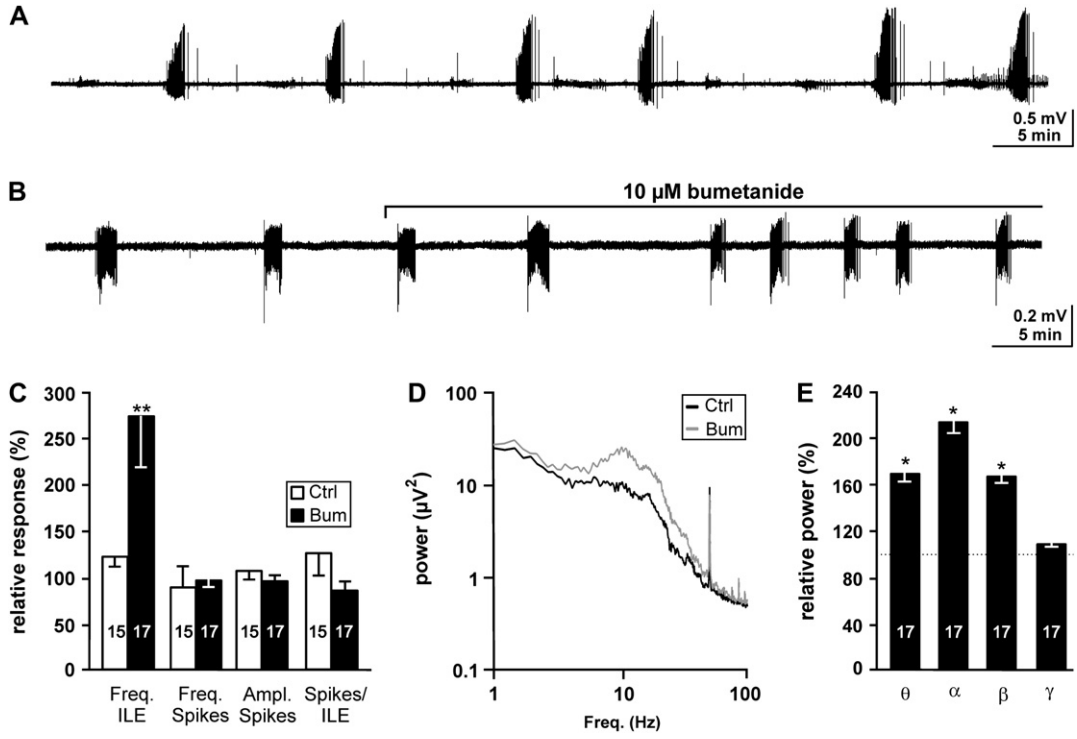

Fig. 5. Effect of bumetanide on epileptiform activity induced by kainate. A: Field potential recording of ictal-like events (ILE) induced by 1 μM kainate in the CA3 region of an intact hippocampal preparation from a P5 mouse. B: Effect of bumetanide on kainate-induced ILE. Application of 10 μM bumetanide increased the frequency of ILE. C: Statistical analysis of the bumetanide effects on different parameters of epileptiform activity. Control experiments (open bars) revealed that the properties of ILE were not significantly altered in the interval used for bumetanide application. Bumetanide (filled bars) significantly increased the frequency of ILE, while the frequency of discharges within an ILE, the amplitude of discharges and the number of discharges per ILE were not significantly affected. D: Power spectrogram of ictal-like activity shown in B before (Ctrl, black line) and during the application of 10 μM bumetanide (Bum, gray line). In the presence of bumetanide an obvious increase in the power was observed. E: Statistical analysis of the relative power, as compared to the control interval before bumetanide application. Bumetanide significantly increased the power in the θ-, α-, and β-frequency range. Bars represent mean ± SEM. Numbers of experiments are indicated in the bars.

and consisted of 6.3 ± 0.6 single discharges with an average amplitude of 104.6 ± 9.9 μV and frequency of 8 ± 0.6 Hz (Fig. 6B).

In the presence of 10 μM bumetanide the number of discharges per LRD was significantly ($p = 0.004$) reduced by 28.1 ± 5.3% ($n = 27$, Figs. 6C,D) and their amplitude was slightly, but significantly ($p = 0.033$) attenuated by 7.5 ± 4.6% (Fig. 6E), while the frequency of LRD (102 ± 4.2%) and the frequency of discharges within an LRD (103 ± 5.6%) were not affected (Fig. 6E). In accordance with this significant decrease in the number of discharges per LRD, the power of epileptiform activity was also reduced by bumetanide (Figs. 6F,G). Bumetanide caused a significant decrease in the power of LRD in all analyzed frequency ranges. In control experiments ($n = 18$) without bumetanide application LRD properties were not significantly affected during the recording interval of 60 min, while a significant ($p < 0.05$) power increase in θ- and α-frequency range occurred over this time (data not shown). In summary these results demonstrate that in the 4-AP/low-Mg^{2+} model bumetanide attenuates LRD-like epileptiform activity.

4. Discussion

The findings of the present study can be summarized as follows: (i) In the CA3 region of P4–P7 mouse whole hippocampal preparations different in-vitro epilepsy models induced epileptiform activity with distinct properties. (ii) Ictal-like activity induced by elevated $[K^+]_e$ was attenuated by bumetanide. (iii) Interictal activity elicited by blockade of $GABA_A$ and glycine receptors was unaffected by bumetanide. (iv) In the low-Mg^{2+} model interictal activity was enhanced by bumetanide, while the ictal-like events were unaffected. (v) Kainate-induced ictal-like activity was enhanced by bumetanide. (vi) In the combined 4-AP/low-Mg^{2+} model, the late recurrent discharges were slightly attenuated by bumetanide. In summary, these results demonstrate that bumetanide did not consistently attenuate epileptiform activity but exerts distinct effects on epileptiform activity in different in-vitro epilepsy models.

The main finding of the present study is that bumetanide has differential effects on epileptiform activity induced by distinct in-vitro epilepsy models. In accordance with previous findings by Dzhala et al. (2005), we observed that bumetanide

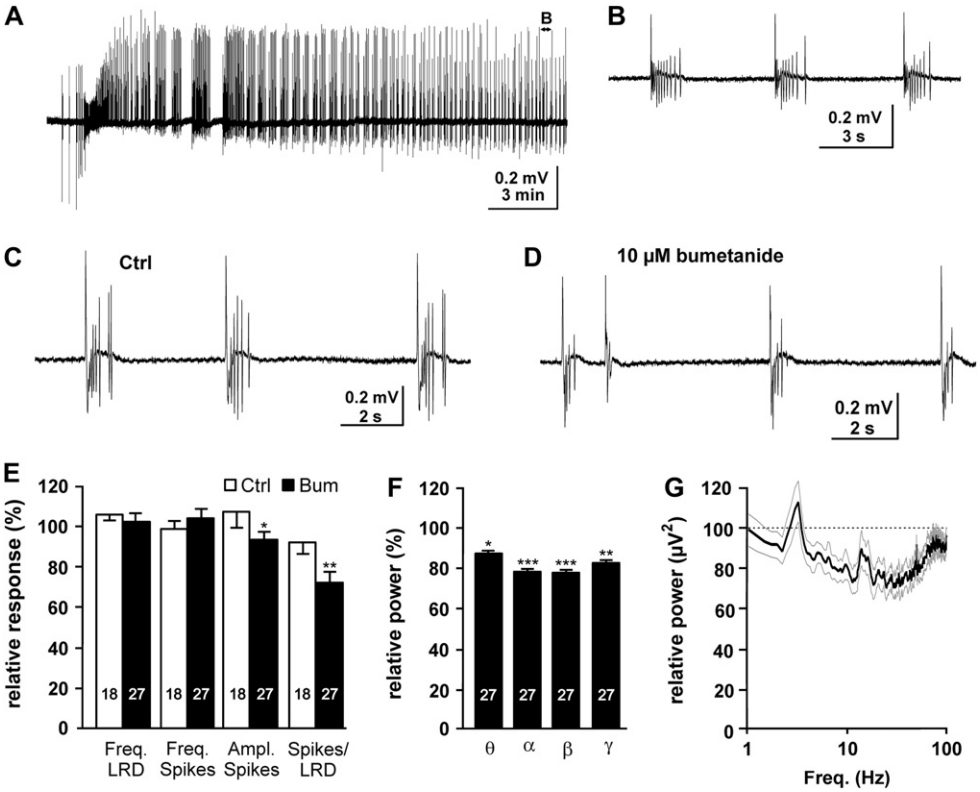

Fig. 6. Effect of bumetanide on epileptiform activity induced by application of 20 μM 4-AP under low-Mg^{2+} conditions. A: Field-potential recording in the CA3 region of a whole-hippocampus preparation from a P7 mouse. Application of 20 μM 4-AP in low-Mg^{2+} solution induced initial ictal-like bursts, followed by late recurrent discharges (LRD). B: Three LRD, as marked in A, displayed at higher temporal resolution. C, D: Subsequent recordings of LRDs induced by 4-AP/low-Mg^{2+} conditions before (Ctrl) and after the application of 10 μM bumetanide. Note that the number of discharges per LRD was reduced in the presence of bumetanide. E: Statistical analysis of bumetanide effects on different LRD parameters. While in control experiments the properties of LRD were unaltered in the interval used for bumetanide application (open bars), bumetanide (filled bars) significantly reduced the number of discharges per LRD and their amplitude. F: Statistical analysis of the relative power, as compared to control experiments before bumetanide application. Bumetanide significantly decreased the power from θ- to γ-frequency range. G: Spectrogram displaying the average relative power of LRD from 27 experiments (thick line ± SEM indicated by thin, gray lines) in the presence of 10 μM bumetanide. Note the reduction in relative power. Bars represent mean ± SEM. Numbers of experiments are indicated in the bars.

attenuated the ictal-like epileptiform activity in the high $[K^+]_e$ model. However, in the whole hippocampal preparation, bumetanide induced a decrease in amplitude and frequency of epileptiform discharges, instead of a switch in the discharge pattern observed in slice preparations (Dzhala et al., 2005). This discrepancy can be explained most likely by differences in functional connectivity between both preparations. Although a general increase in excitation underlies the ictal-like epileptiform activity observed under elevated $[K^+]_e$ (McBain, 1994; Dzhala and Staley, 2003), an altered Cl^- homeostasis due to a decreased electromotive force for K^+-Cl^- cotransport may also contribute to seizure generation (Korn et al., 1987). Therefore an artificial elevation of $[Cl^-]_i$ and a corresponding positive shift in E_{GABA} can not be excluded in the high $[K^+]_e$ model. Hence, the suppressing effect of bumetanide on epileptiform activity may only be observed under elevated $[K^+]_e$ conditions.

To investigate this possibility, we used other epilepsy models that do not artificially enhance $[K^+]_e$ and probably do not interfere with Cl^- transport processes. We found that ictal-like events were hardly affected in the low-Mg^{2+} model, indicating that ictal-like activity was not attenuated per-se by bumetanide. To support this finding we also used the kainate-model as a third in-vitro model of ictal-like activity. These experiments revealed that bumetanide can even enhance ictal-like activity. In summary, these experiments clearly show that the suppressing effect of bumetanide on ictal-like activity critically depends on the model used.

Because interictal activity induced by $GABA_A$ receptor blockade was not affected by bumetanide, Dzhala et al. (2005) suggested that the bumetanide effect was mediated via $GABA_A$ receptors. In accordance with their results, we also found that bumetanide only slightly affected the interictal-like epileptiform events induced by the complete block of ligand-gated Cl^- channels. The only significant effect was a slight decrease in discharge amplitude, which may be caused by a non-synaptic effect of bumetanide (Sykova, 2004). However, to address the question whether the lack of bumetanide effect in the disinhibition model really indicates that ligand-gated Cl^- channels are required to mediate its anticonvulsant action, we investigated an additional model of interictal-like activity. We found that bumetanide slightly enhanced the power of interictal-like activity in the low-Mg^{2+} model, indicating that in the presence of functional ligand-gated Cl^- channels bumetanide still did not attenuate interictal-activity. Thus, the lack of bumetanide effects on the interictal-activity in the disinhibition model did not necessarily indicates that ligand-gated Cl^- channels are required to mediate the attenuating effect of bumetanide.

In contrast to the findings that bumetanide enhanced epileptiform-discharges in the kainate and the low-Mg^{2+} model, epileptiform-activity was attenuated in the 4-AP/low-Mg^{2+} model. In this model the attenuation of power corresponds to the significant reduction in the number of discharges per burst. On the contrary, the enhancement of low-Mg^{2+} induced interictal-like activity in the β-frequency range corresponds to in increase in the number of discharges within an interictal burst. Since the repetitive spikes following the initial discharge represents synchronized synaptic interactions (Miles et al., 1984), a change in the number of discharges per burst indicates that bumetanide may influence synaptic interactions. One possible explanation for the different effects of bumetanide on the number of discharges per epileptiform burst is that interictal bursts and LRD are maintained by distinct synaptic networks, which are differentially influenced by bumetanide. This possibility is supported by the finding, that interictal bursts and LRD have a distinct pharmacology (Zhang et al., 1994). On the other hand, we can not exclude that the repetitive discharges during LRD will increase $[K^+]_e$ (Hablitz and Heinemann, 1987) and thus affect $[Cl^-]_i$ homeostatic processes (Korn et al., 1987).

In summary, the experiments performed in the present study demonstrate that the suppressing effect of bumetanide on ictal-like epileptiform activity critically depends on the model used and that in some models epileptiform activity may also be enhanced by bumetanide. However, this enhanced epileptiform activity in in-vitro models does not necessarily imply that bumetanide exerts proepileptogenic effects in-vivo. The effect of bumetanide is not necessarily mediated by alterations in Cl^- homeostasis. One major function of bumetanide-sensitive Na^+-dependent K^+-$2Cl^-$ cotransport is the control of plasma osmolarity via its central role in renal secretion. Bumetanide induces diuresis thereby leading to hyperosmotic dehydration which in turn increases the size of the extracellular space (Sykova, 2004). Hence, under in-vivo conditions bumetanide may mediate its effects by targets outside the CNS, in particular as experimental data suggest that bumetanide only poorly crosses the blood–brain barrier (Javaheri et al., 1993). Even in an in-vitro situation bumetanide may alter extracellular space, because NKCC1 is one major element of cellular volume regulation (Russell, 2000). An effect of bumetanide on the extracellular volume fraction must thus be considered under in-vivo and in-vitro conditions, because changes in the extracellular volume fraction affect epileptiform activity in a variety of preparations including the immature hippocampus (Sykova, 2004; Kilb et al., 2006). Therefore, bumetanide-induced alterations of the extracellular space or other non-synaptic effects may contribute to its soothing effect on in-vitro and in-vivo neonatal seizures, as has already been proposed by Fukuda (2005).

Acknowledgments

This study was supported by DFG grant Ki 835/2-1 to WK. The authors thank D. Richter for performing some of the experiments.

References

Baram, T.Z., Snead III, O.C., 1990. Bicuculline induced seizures in infant rats: ontogeny of behavioral and electrocortical phenomena. Dev. Brain Res. 57, 291–295.

Dulac, O., Macdonald, R.L., Kelly, K.M., 1995. Age-specific antiepileptic drug treatment and development of age-specific antiepileptic drugs. In: Schwartzkroin, P.A., Moshe, S.L., Noebels, J.L., Swann, J.W. (Eds.), Brain

Development and Epilepsy. Oxford Univ. Press, New York & Oxford, pp. 289–326.

Dzhala, V.I., Staley, K.J., 2003. Transition from interictal to ictal activity in limbic networks in vitro. J. Neurosci. 23, 7873–7880.

Dzhala, V.I., Talos, D.M., Sdrulla, D.A., Brumback, A.C., Mathews, G.C., Benke, T.A., Delpire, E., Jensen, F.E., Staley, K.J., 2005. NKCC1 transporter facilitates seizures in the developing brain. Nat. Med. 11, 1205–1213.

Fukuda, A., 2005. Diuretic soothes seizures in newborns. Nat. Med. 11, 1153–1154.

Hablitz, J.J., Heinemann, U., 1987. Extracellular K+ and Ca2+ changes during epileptiform discharges in the immature rat neocortex. Dev. Brain Res. 36, 299–303.

Holmes, G.L., 1997. Epilepsy in the developing brain: lessons from the laboratory and clinic. Epilepsia 38, 12–30.

Holmes, G.L., Khazipov, R., Ben Ari, Y., 2002. New concepts in neonatal seizures. Neuroreport 13, A3–A8.

Javaheri, S., Davis, C., Rogers, D.H., 1993. Ionic composition of cisternal CSF in acute respiratory acidosis: lack of effect of large dose bumetanide. J. Neurochem. 61, 1525–1529.

Khalilov, I., Esclapez, M., Medina, I., Aggoun, D., Lamsa, K., Leinekugel, X., Khazipov, R., Ben Ari, Y., 1997a. A novel in vitro preparation: the intact hippocampal formation. Neuron 19, 743–749.

Khalilov, I., Khazipov, R., Esclapez, M., Ben Ari, Y., 1997b. Bicuculline induces ictal seizures in the intact hippocampus recorded in vitro. Eur. J. Pharmacol. 319, R5–R6.

Khalilov, I., Dzhala, V., Medina, I., Leinekugel, X., Melyan, Z., Lamsa, K., Khazipov, R., Ben-Ari, Y., 1999. Maturation of kainate-induced epileptiform activities in interconnected intact neonatal limbic structures in vitro. Eur. J. Neurosci. 11, 3468–3480.

Kilb, W., Dierkes, P.W., Sykova, E., Vargova, L., Luhmann, H.J., 2006. Hypoosmolar conditions reduce extracellular volume fraction and enhance epileptiform activity in the CA3 region of the immature rat hippocampus. J. Neurosci. Res. 84 (1), 119–129.

Kirchner, A., Breustedt, J., Rosche, B., Heinemann, U.F., Schmieden, V., 2003. Effects of taurine and glycine on epileptiform activity induced by removal of mg2+ in combined rat entorhinal cortex-hippocampal slices. Epilepsia 44, 1145–1152.

Korn, S.J., Giacchino, J.L., Chamberlin, N.L., Dingledine, R., 1987. Epileptiform burst activity induced by potassium in the hippocampus and its regulation by GABA-mediated inhibition. J. Neurophysiol. 57, 325–340.

Luhmann, H.J., Prince, D.A., 1991. Postnatal maturation of the GABAergic system in rat neocortex. J. Neurophysiol. 65, 247–263.

McBain, C.J., 1994. Hippocampal inhibitory neuron activity in the elevated potassium model of epilepsy. J. Neurophysiol. 72, 2853–2863.

Miles, R., Wong, R.K.S., Traub, R.D., 1984. Synchronized after discharges in the hippocampus: contribution of local synaptic interactions. Neuroscience 12, 1179–1189.

Moser, J., Kilb, W., Werhahn, K.J., Luhmann, H.J., 2006. Early developmental alterations of low-Mg2+-induced epileptiform activity in the intact corticohippocampal formation of the newborn mouse in vitro. Brain Res. 1077, 170–177.

Rohrbough, J., Spitzer, N.C., 1996. Regulation of intracellular Cl− levels by Na(+)-dependent Cl− cotransport distinguishes depolarizing from hyperpolarizing $GABA_A$ receptor-mediated responses in spinal neurons. J. Neurosci. 16, 82–91.

Russell, J.M., 2000. Sodium-potassium-chloride cotransport. Physiol. Rev. 80, 211–276.

Sanchez, R.M., Jensen, F.E., 2001. Maturational aspects of epilepsy mechanisms and consequences for the immature brain. Epilepsia 42, 577–585.

Sykova, E., 2004. Extrasynaptic volume transmission and diffusion parameters of the extracellular space. Neuroscience 129, 861–876.

Wells, J.E., Porter, J.T., Agmon, A., 2000. GABAergic inhibition suppresses paroxysmal network activity in the neonatal rodent hippocampus and neocortex. J. Neurosci. 20, 8822–8830.

Yamada, J., Okabe, A., Toyoda, H., Kilb, W., Luhmann, H.J., Fukuda, A., 2004. Cl− uptake promoting depolarizing GABA actions in immature rat neocortical neurones is mediated by NKCC1. J. Physiol. 557, 829–841.

Zhang, C.L., Gloveli, T., Heinemann, U., 1994. Effects of NMDA- and AMPA-receptor antagonists on different forms of epileptiform activity in rat temporal cortex slices. Epilepsia 35 (Suppl. 5), S68–S73.